論文 한국정밀공학회지 제13권 제11호 (1996년 11월)
Journal of the Korean Society of Precision Engineering Vol. 13. No 11. NOVEMBER. 1996.

SRIM/RIM을 위한 공정 인자의 수치 해석적 평가

이 중 희*, Robert J. Duh**

Computational Estimation of Process Parameters in Structural Reaction Injection Molding

Joong-Hee Lee*, Robert J. Duh**

ABSTRACT

Structural reaction injection molding을 이용한 복합재료의 제품 성형을 위한 모델링 전략을 설명하였다. 사용된 모델은 두 평행한 원판형 mold에 있는 불 균일한 온도조건의 fiber preform을 통과하는 reactive resin의 방사형 유동을 시뮬레이션 한다. 이러한 모델은 중요한 작동인자와 공정인자(주입온도, mold의 온도, 유량, cavity의 두께와 섬유의 조밀도)등이 유동속도, 변환(monomer, radical, inhibitor) 및 온도분포 등에 미치는 영향을 예견한다. 열전달과 질량전달 및 화학반응을 고려하여 모델을 개발하였다. 중요한 공정인자를 평가하기 위한 효율적인 공정창(process window)을 제공하는데 본 연구의 목적을 두었다. 2차원적인 Lagrangian 방식에 1차원적인 유동과 제한적인 2차원 열전달을 가정하여 모델을 유도하였고, 방정식은 implicit difference scheme에 의해 전개하였다. 이 모델은 Gonzalez-Romero의 실험 결과와 비교함에 의해 확인되었고, 실험결과가 잘 일치함을 보였다.

Key Words: reaction injection molding(반응식 사출성형), finite difference scheme(유한 급차법), constant volumetric flow rate(정적 유동비), computational process window(수치적 공정 상태도)

1. Introduction

Structural reaction injection molding (SRIM), and its lower speed relative, resin transfer molding (RTM), are being widely recognized as holding a great potential for increased use in the production of composite parts. SRIM has received attention especially in the ground vehicle industry, where there is considerable interest in obtaining the benefits of polymer composite materials with low cost and high volume production rates. Benefits of SRIM/RTM processing include the ability to produce reduced weight replacements in existing applications and to reduce manufacturing cost due to part consolidation[1]. The advantages of SRIM processing in comparison with thermoplastic injection molding are shared with reaction injection molding (RIM), and include low process-

* 전북대학교 신소재공학부
** Mechanical Engineering, University of Minnesota

ing temperature, and reduced clamping pressure requirements[2 3 4 5].

In recent years, a number of authors have presented models capable of handling two and three dimensional flows[6]. One aspect of the modeling that has been identified as being important for the production of large parts is the ability to anticipate premature gelation. Experimental results reported by Scrivo[5], for example, document the effect of mold temperature on the incomplete filling of large parts due to premature gelation. To predict this numerically requires simultaneously calculating flow, heat transfer, and chemical reaction instead of assuming that the reaction begins after filling is complete, as is done by Gonzalez-Romero[2, 7].

Because of the complex thermal-chemical interactions inherent in SRIM, existing models require long computing time even when ignoring chemical reaction during the filling stage. The objective of this research is to develope a methodology for obtaining limits on important process variables within which successful parts may be produced. Moreover, a more numerically efficient simulation of SRIM which captures the important features is desired. A modeling strategy which achieves this objective and can be used to give reasonable guidelines for SRIM process design is presented. The numerical simulations are verified by comparison with experimental results published by Gonzalez-Romero[7] and found to be in good agreement. Finally, a sample process window is computed using this model for mold temperature and initial (inlet) material temperature.

2. Mathematical Model

Since the objective of the model is not an accurate prediction of the flow front, but rather a reasonable prediction of whether the part will fill and cure successfully, one dimensional radial flow between parallel plates is assumed. With this assumption, a Lagrangian framework is employed, in which the coordinate system is fixed on a particle as it moves radially outward. Since the field variables are symmetric about the midplane of the mold, the solution is sought between the midplane and the top of the mold. A finite-difference scheme is used to discretize both time and space.

This work is based on the conservation of volume and energy. Emphasis is placed on making appropriate assumptions to simplify the calculations while representing the major feature of the process. The equations are expressed in terms of temperature.

2.1 Basic Assumptions

In SRIM as shown in Figure 1, the thickness of mold cavity is usually small. This combined with the resistant pressure of fiber is assumed to result in a flow front with a flat profile[8]. The range of the temperature variation is assumed to be small enough (21℃ to 250℃ in this study) that the thermal conductivity k, the heat capacity C, and the density ρ do not depend on temperature. The fluid is assumed to be incompressible and body forces are neglected. The heat transfer in the radial direction is considered negligible in comparison with the heat transfer in the transverse direction because the mold cavity is thin and the corresponding temperature gradients are much greater in the transverse direction.

Heat transfer between the polymer and the fiber preform is assumed to occur on a much shorter time scale than that between the polymer and mold due to the large surface area of the fibers. As in the example of Gonzalez-Romero[7], the temperature of the fiber and the polymer are assumed to reach equilibrium within one time step after the polymer reaches the fiber. Based on the conservation of energy, this equilibrium temperature can be obtained by:

$$T = \frac{m_p C_p T_p + m_f C_f T_f}{m_p C_p + m_f C_f} \quad (1)$$

where m_p is the mass of polymer, m_f is the mass of fiber, C_p is the heat capacity of polymer, C_f is the heat capacity of fiber, T_p is the temperature of polymer, T_f is the temperature of fiber, and T is the equilibrium temperature of the polymer/fiber. The properties of the polymer/fiber are obtained using a harmonic average:

$$C = \frac{m_p C_p + m_f C_f}{m_p + m_f} \quad (2)$$

$$k = \frac{k_p k_f}{(1-\Phi)k_p + \Phi k_f} \quad (3)$$

$$\rho = \Phi\rho_p + (1-\Phi)\rho_f \quad (4)$$

where C is the heat capacity of the polymer/fiber composite, k, k_p, and k_f are the thermal conductivities of the polymer/fiber composite, polymer, and fiber respectively, ρ, ρ_p and ρ_f are the densities of the polymer/fiber composite, polymer, fiber respectively, and Φ is the porosity which is the volume fraction of the polymer. The values of these thermal properties are listed in Table 1.

2.2 Governing Equations

The conservation of energy leads to the heat equation for a given material

$$\rho C \frac{\partial T}{\partial t} = k \frac{\partial^2 T}{\partial y^2} + \dot{q} \quad (5)$$

where t is time and y is the dimension in the transverse direction, and $\dot{q}$ is the heat generation rate. The initial conditions can be obtained from Equation (1) by substituting $T_f = T_m$ and $T_p = T_o$, $T_m$is the mold temperature and T_o is the initial temperature of polymer. The boundary conditions are:

$$k \frac{\partial^2 T}{\partial y^2}\bigg|_{y=\frac{H}{2}} = \begin{cases} \frac{h}{\Delta y}[T_m - T]_{y=\frac{H}{2}} & during\ filling \\ \frac{k_b}{\Delta y^2}[T_m - T]_{y=\frac{H}{2}} & during\ curing \end{cases} \quad (6)$$

$$\frac{\partial T}{\partial y}\bigg|_{y=0} = 0 \quad (7)$$

where h is the heat transfer coefficient, and k_b is the boundary thermal conductivity at the wall between mold and polymer. The value of h is based on the radial velocity of polymer, v_r as described by Gonzalez-Romero[7]:

$$h = \lambda v_r \quad (8)$$

where λ is the heat transfer coefficient constant with the value given in Table 1. The boundary thermal conductivity k_b is given by:

$$k_b = \frac{2kk_m}{k + k_m} \quad (9)$$

Based on conservation of volume, the continuity equation is

$$Q = \int_{-\frac{H}{2}}^{\frac{H}{2}} 2\pi\Phi r v_r dy \quad (10)$$

where Q is the flow rate, r is the radial position, H is the mold thickness, and v_r is the velocity in radial direction.

Table 1: Thermal Properties from Gonzalez-Romero [7].

Parameter	Value
ρ_f (g/cm^3)	1.1
ρ_f (g/cm^3)	2.54
C_p (cal/g ℃)	0.45
C_f (cal/g ℃)	0.2
k_p (cal/sec cm^3)	0.0004
k_f (cal/sec cm^3)	0.0016
k_m (cal/sec cm^3)	0.56
λ (cal/°K cm^3)	1.0468×10^{-5}

2.3 Numerical Scheme

During the filling stage, each polymer segment moves out like a circular ring as the mold is filled. For a constant flow rate mold filling, one dimensional flow assumption means that the location of the flow front does not need to be found numerically but can be calculated directly from Equation (10) at any point in time. As described above, the heat transfer within the Lagrangian framework is assumed to be 1-dimensional in the transverse direction(no radial conduction), and the symmetry with respect to the midplane of the mold reduces the calculation domain to one half of the mold thickness.

Each circular ring of the polymer/fiber composite is divided into several segments in the y-direction; ten segments were used for the results reported. Unconditional stability was achieved by implementing a fully implicit numerical scheme, with backward differences in time and central differences in space used to discretize the governing equation. In this approach, the calculations for heat conduction are based on the unknown current temperatures, while the temperature of the material at the end of the previous time step is used in the solution of the kinetic equations to calculate the heat generation term.

Using the first subscript to represent time and the second subscript to represent the position in the y-direction, the governing equation can be expressed as:

$$T_{i,j} - T_{i-1,j} = \frac{k\Delta t}{\rho C \Delta y^2}[T_{i,j+1} + T_{i,j-1} - 2T_{i,j}] + \frac{\Delta t}{\rho C}\dot{q}(T_{i-1,j}) \quad (11)$$

where Δt is the time step and Δy is the thickness in y-direction of each segment. The subscript j ranges from 1 at the mold wall to N at the midplane, while i varies from 1 for the first material entering the mold to M for the last.

Considering symmetry about the mold midplane, the governing equation at the center of the cavity can be written as:

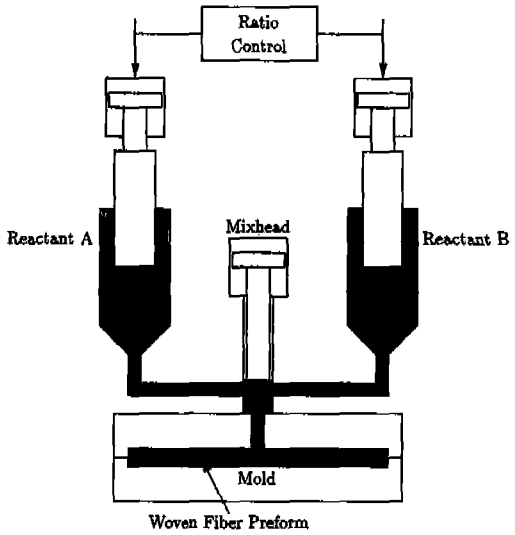

Fig.1 Schematic diagram of Structural Reaction Injection Molding.

$$T_{i,N} - T_{i-1,N} = 2\beta[T_{i,N-1} - T_{i,N}] + \frac{\Delta t}{\rho C}\dot{q}(T_{i-1,N}) \quad (12)$$

where β *is* $\frac{k\Delta t}{\rho C \Delta y^2}$.

At the mold wall, the governing equation can be written:

$$T_{i,1} - T_{i-1,1} = \beta_m[T_m - T_{i,1}] - \beta[T_{i,1} - T_{i,2}] + \frac{\Delta t}{\rho C}\dot{q}(T_{i-1,1}) \quad (13)$$

where β_m is

$$\beta_m = \begin{cases} \frac{h\Delta t}{\rho C \Delta y} & during\ filling \\ \frac{k_b \Delta t}{\rho C \Delta y^2} & during\ curing \end{cases} \quad (14)$$

This numerical scheme converges with a relatively large time step as shown in Fig. 2 plotted the calculated gelation time as a function of the

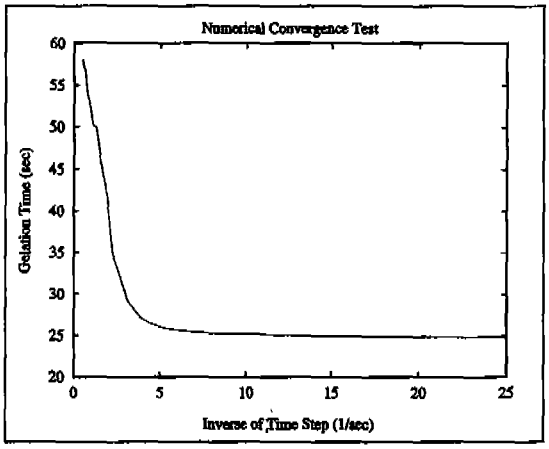

Fig. 2 Predicted gelation time as a function of numerical time step for conditions corresponding to Experiment 1 in Table 2.

inverse time step. Based on these results, a time step of 0.1 seconds was selected for subsequent calculations. An important advantages of a large time step is that, since one ring of material elements is assumed to enter the mold during each time step, the number of material elements is reduced. Thus in this scheme the memory requirements are proportional to the inverse time step.

A further numerical simplification employed based on the stated assumptions allows the tracking of only the material point or points of interest once filling is complete. Since filling is usually a small fraction of the total simulation time, this allows tremendous additional time savings when only one or a few locations contain information of interest.

2.4 Material Tracking

A constant volumetric flow rate was modeled in order to compare with the experimental results from Gonzalez-Romero[7]. Using the flow rate, the radial position, r can be obtained by conservation of volume:

$$r = \left[\frac{\int_0^t Q dt}{\pi H}\right]^{\frac{1}{2}} \tag{15}$$

The radial position is used to trace each polymer particle. The average velocity in radial direction from time t_{i-1} to time t_i can be obtained from the material element's radial position r:

$$v_r = \frac{r_i - r_{i-1}}{\Delta t} \tag{16}$$

The velocity v_r is necessary for calculating the heat transfer coefficient h.

3. Model Verification

In order to verify this model, analytical predictions were compared with experimental results from Gonzalez-Romero[7]. The circular mold cavity between the midplane and the mold wall was divided into ten segments in the transverse direction. The various experimental conditions are summarized in Table 2.

Table 2: Experimental Conditions from Gonzalez-Romero[7]

Parameter	Exp. 1	Exp. 2	Exp. 3
R_m (cm)	10	10	10
H (cm)	0.58	0.63	0.53
ϕ	0.764	0.764	0.764
Q (cm^3/sec)	22	25	28
T_o (°K)	297	294	300
T_m (°K)	411	399	415
r^* (cm)	3.2	3.2	3.2
ζ^*	0.1	0.1	0.1

* sensor location

3.1 Polymerization Kinetics

A styrene-dimethacrylate copolymer material model based on Gonzalez-Romero's work has been incorporated into this analysis. This polymerization system contained equal amounts, by mass, of ethoxylated bisphenol A dimethacrylate and styrene. The resin also contained 1% by weight of paratertiary butyl peroxide used as a free radical initiator, and an undetermined amount of hydroquinone which is contained as an inhibitor in the commercial resin. The inhibitor was used to delay reaction during the filling stage, and to reduce the risk of excessively high temperature during curing which can degrade the material. The material reacts via free radical co-polymerization, setting its shape by crosslinking. The chemical system is referred to as a styrene-dimethacrylate (SDM) copolymer.

The heat generation rate, $\dot{q}$, is given by the following equations:

$$\dot{q} = \Phi \Delta H_r \frac{\partial X}{\partial t} \tag{17}$$

$$\Delta H_r = \rho C_p T_{ad} \tag{18}$$

where Φ is the porosity, ΔH_r is the chemical heat of reaction, X is the conversion of monomer, ρ is the density of resin, C_p is the heat capacity, and T_{ad} is the adiabatic temperature rise, which for this system was reported to be 162 °K. There are three species in this chemical system: the monomer, the radicals, and the inhibitor. The equations of species balance are given by the following set of equations, where R^* is the conversion of radicals, and Z^* is the conversion of inhibitor:

Monomer

$$\frac{\partial X}{\partial t} = k_X R^* [1 - X] \tag{19}$$

Radicals

$$\frac{\partial R^*}{\partial t} = 1 - k_X t_Z \frac{k_Z}{k_p} [1 - Z^*] R^* \tag{20}$$

Inhibitor

$$\frac{\partial Z^*}{\partial t} = k_X \frac{k_Z}{k_p} [1 - Z^*] R^* \tag{21}$$

Table 3: Kinetic Parameters from Gonzalez-Romero[7]

Parameter	Value
$t_z(sec^{-1})$	$B_1\ exp(B_2/T)$
$k_X(sec^{-1})$	$A_X\ exp(-E_X/T)$
k_z/k_p	25
$A_X(sec^{-2})$	1.15×10^6
$E_X(°K)$	-9.0×10^3
$B_1(sec^{-1})$	2.05×10^{-20}
$B_2(°K)$	1.91×10^4

The initial conditions for all of these three species are zero. The parameters in the above equations were obtained by fitting experimental data and are reproduced in Table 3. The value reported for E_x in the table has been rounded off, from about -8630 °K to -9000 °K, improving the agreement for all cases tested. This liberty was taken because there exists considerable uncertainty in extrapolating the temperature dependence represented by this parameter from the 7 °K range over which the kinetic data were fit.

For this polymer system, when the conversion of monomer reaches approximately 64%, the polymer begins to gel[7]. The viscosity of the polymer increases rapidly and as a result the flow is stopped. If this conversion level is reached during the filling stage, the filling process will cease resulting in an incompletely molded part. In the

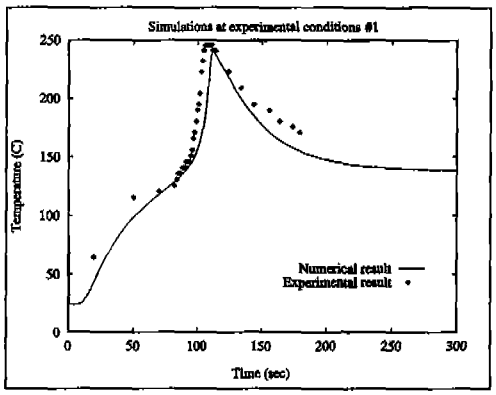

Fig. 3 Comparison of predicted and experimental temperature histories for one sensor, corresponding to the conditions of Experiment 1 in Table 2.

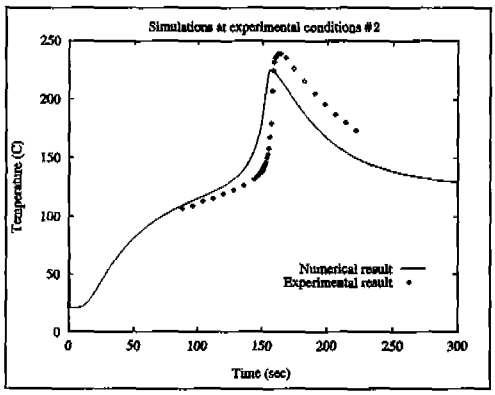

Fig. 4 Comparison of predicted and experimental temperature histories for one sensor, corresponding to the conditions of Experiment 2 in Table 2.

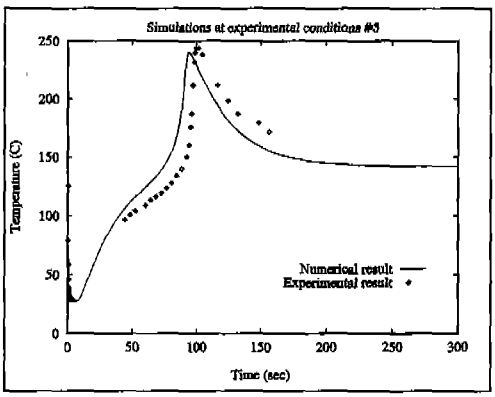

Fig. 5 Comparison of predicted and experimental temperature histories for one sensor, corresponding to the conditions of Experiment 3 in Table 2.

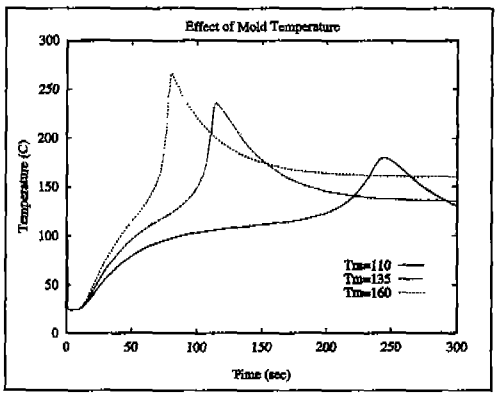

Fig. 6 Predicted in-mold temperature history corresponding to Experiment 1 in Table2, with various mold temperatures.

numerical model, this condition is checked to flag unsuitable molding conditions.

4. Discussion

The predicted temperature profiles and corresponding experimental data from Gonzalez-Romero for experimental conditions 1-3 are plotted in Figures 3-5. In these plots, $\xi(=2y/H)$ is the dimensionless transverse position, where H is the total mold thickness. On a 60 MHz 486-based PC with a math co-processor, the simulation required only 11 seconds, where the temperature at a single location of interest was computed for 300 seconds of simulated time. The agreement between the numerical predictions and the experimental results is very good overall. For the remainder of the comparisons, the excellent agreement suggests that the simplifying assumptions did not omit important features in modeling the process. When the temperature of this resin reaches 60-80℃, the reaction rate increases sharply[9]. After this point, the polymer temperature becomes higher than the mold temperature and the mold becomes a cooling system, helping to prevent material degradation, or possibly quenching the reaction and preventing complete

cure: The material at the center gels and reaches its peak temperature earlier than the material at the walls.

The predicted effect of mold temperature is illustrated in Figure 6, based on the conditions for experiment 1 in Table 2. For this set of conditions, the model predicts that the reaction will not go to completion when the mold temperature is below 107℃. In contrast, when the mold temperature is above 230℃, the mold will not be completely filled because of premature gelation. It can be seen from the numerical results that a 10 ℃ change in mold temperature would be expected to reduce the cycle time by about 50%. The peak

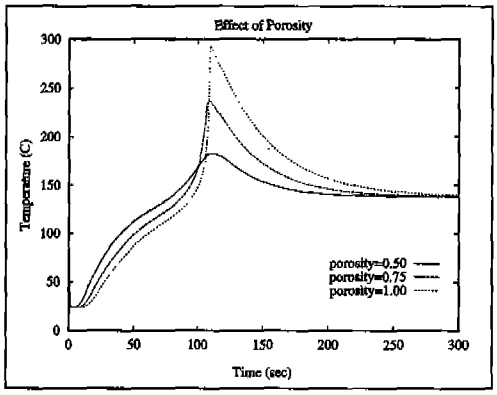

Fig. 7 Predicted in-mold temperature history corresponding to Experiment 1 in Table2, with various fiber preform porosities.

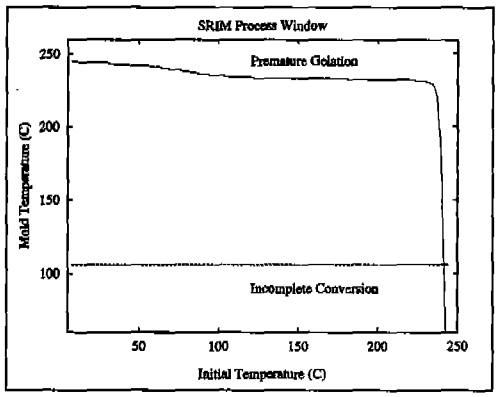

Fig. 8 Predicted premature and incomplete chemical reaction for thickness, porosity, and flow rate corresponding to Experiment 1 in Table2, with variable mold and initial resin temperature.

temperatures are also significantly changed, implying a change in glass transition temperature.

The predicted effect of fiber volume fraction on temperature exotherms is shown in Fig. 7. The fiber volume fraction affects the temperature in several ways. With increased volume fraction, the velocities are higher for the same input flow rate. More heat is transferred from the preform to the polymer because of the increased thermal capacity of the glass preform, and this heat is transferred to less polymer, increasing its temperature more rapidly. During the reaction, the increased fiber volume fraction reduces the volume fraction of polymer capable of generating heat. Finally, the thermal conductivity of the system is increased. These effects can be observed in the temperature profiles shown in the figure. Before the major reaction takes place, the composite with more fiber($\phi = 0.5$) heats up faster than the pure resin($\phi = 1.0$), and as a result the reaction begins sooner. After the polymer temperature exceeds the mold temperature, the increased fiber content increases the heat transfer from the polymer to the mold and reduces the total heat generated, slowing down the reaction and resulting in a lower peak temperature.

To illustrate the application of this model to the determination of a process window, the effects of the mold temperature and initial are considered simultaneously in Fig. 8. These numerical results can provide the basis for adjusting the process variables to avoid incomplete chemical reaction, incomplete filling and material degradation. A complete SRIM process design requires choosing the initial temperature and mold temperature inside these margins.

5. Conclusion

A model has been presented for study of the coupled phenomena of flow, chemical reaction,

and heat transfer during SRIM. The one-dimensional model is capable of quickly producing moldability information for such process parameters as mold temperature, initial temperature, and fiber volume fraction. Different chemical kinetics may be easily incorporated to explore different polymer systems. An example process window for initial resin temperature and mold temperature limits is presented.

The implicit finite difference scheme employed in this model allowed the use of a relatively large time step, resulting in a solution that is considerably more computationally efficient than a fully explicit scheme and slightly better than a Crank-Nicholson formulation. A typical simulation required 11 seconds on a 60 MHz 486-based personal computer.

A further application envisioned for this model is in parameter estimation studies. In many cases some process parameters such as heat transfer coefficients or certain kinetics parameters may be very difficult to obtain experimentally. In such cases, an inverse problem methodology may be devised which uses a numerically efficient model like the one presented here to estimate these difficult to measure properties.

References

1. Hansen, R. S., "RTM Processing and Applications," *SME Technical Paper EM90-214*, 1990.
2. Gonzalez-Romero, V. M. and Macosko, C. W., "Process Parameters estimation for structural reaction injection molding and resin transfer molding," *Polymer Engineering and Science*, Vol. 30, pp. 142-146, 1990.
3. Lakakou, C. N. and Richardson, S. M., "Simulation of reacting flow during filling in reaction injection molding(rim)," *Polymer Engineering and Science*, Vol. 26, pp. 1264-1275, 1986.
4. Molnar, J. A., Trevino, L., and Lee, L. J., "Molding filling in srim and rtm: controlling a critical processing parameter," *Modern Plastics*, Vol. 66, pp. 120-126, 1989.
5. Scrivo, J. V., "It pays to mold large parts from rim structural foam," *Plastics Engineering*, Vol. 40, pp. 67-72, 1984.
6. Hays, R. E., Dannelongue, H. H., and Tanguy, P. A., "Numerical simulation of mold filling in reaction injection molding," *Polymer Engineering and Science*, Vol. 31, pp. 842-848, 1991.
7. Gonzalez-Romero, V. M., Studies of Reactive Polymer Processing with Fiberglass Reinforcement, PhD thesis, University of Minnesota, 1983.
8. Kamal, M. R., Goyal, S. K., and Chu, E., "Computer simulation of injection mold filling of viscoelastic polymer with fountain flow," *AIChE Journal*, Vol. 34, pp. 94-106, 1988.
9. Vespoli, N. P. and Alberino, L. M., "Computer modeling of the heat transfer processes and reaction kinetics of urethane-modified isocyanurate rim system," *Polymer Process Engineering*, Vol. 3, pp. 127-147, 1985.